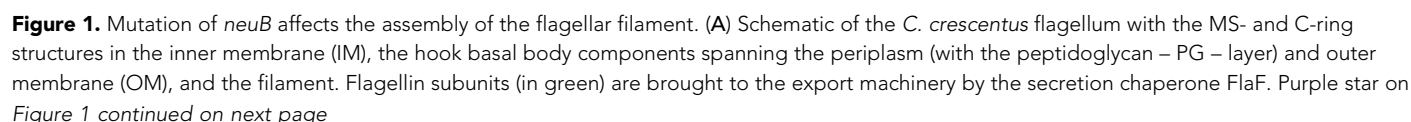


---

## Figures and figure supplements

Specificity in glycosylation of multiple flagellins by the modular and cell cycle regulated glycosyltransferase FlmG

**Silvia Ardisson *et al***



## Figure 1 continued

flagellins indicates the post-translational modification by glycosylation. (B) Schematic of the *C. crescentus* cell cycle. The grey bar represents the time during the cell cycle when CtrA is present and activate transcription of flagellar genes. The hook structure (FlgE, in red) is synthesized in early pre-divisional cells, whereas the flagellar filament (in green) is polymerized from flagellins in late pre-divisional cells. Both, flagellar filament and hook, are shed during the swarmer (SW) to stalked (ST) cell transition. (C) Motility assay of *neuB*::Tn and  $\Delta$ *neuB* mutants compared to WT strain. Overnight cultures were spotted on PYE soft agar plates and incubated for 72 hours at 30°C. Compact swarms indicate that *neuB* mutant cells are non-motile. (D) WT and *neuB*::Tn cells analyzed by transmission electron microscopy show that only a short protrusion is visible at the SW pole of *neuB*::Tn cells, in contrast to the WT strain (black arrow). The images suggest that in *neuB* mutant cells the flagellar hook is stably assembled, but not the flagellar filament. (E) Immunoblots performed with anti-FljK ( $\alpha$ FljK, raised against FljK produced in *E. coli*, see methods) and anti-FlgE (Hahnenberger and Shapiro, 1987) antibodies on cell lysates and supernatants of WT and  $\Delta$ *neuB* cultures show that flagellins are produced in  $\Delta$ *neuB* cells but not efficiently exported, whereas the export of the FlgE hook protein is not affected. The migration of FljK in  $\Delta$ *neuB* cells is shifted towards lower molecular mass, suggesting that post-translational modification of flagellin is defective in the  $\Delta$ *neuB* mutant. Molecular size standards are indicated by the blue lines with the corresponding value in kDa. (F) Immunoblot performed on extracts from *E. coli* cells expressing *C. crescentus* FljK under control of  $P_{lac}$  from a plasmid. FljK expressed in *E. coli* shows the same migration profile as in  $\Delta$ *neuB* cells, indicating that *E. coli* cells cannot post-translationally modify *C. crescentus* FljK. Molecular size standards are indicated by the blue lines with the corresponding value in kDa. Note that antibodies used in this immunoblot were raised against flagellins purified from *C. crescentus* ( $\alpha$ Flagellins; Hahnenberger and Shapiro, 1987). (G) Immunoblots on extracts from  $\Delta$ *flj*<sup>x6</sup> (x6) and  $\Delta$ *flj*<sup>x6</sup> $\Delta$ *neuB* (x6/B) cells expressing each flagellin from a plasmid under  $P_{xyI}$  control. The immunoblots were performed with antibodies raised against purified *C. crescentus* flagellins (upper panel) or FljK expressed and purified from *E. coli* (lower panel). In both cases, all six flagellins show a shift to a lower molecular mass in their migration in the absence of *neuB*, suggesting that all six flagellins are post-translationally modified. Molecular size standards are indicated by the blue lines with the corresponding value in kDa. Both antibodies recognize all six flagellins. Note that antibodies raised against flagellins purified from *Caulobacter* recognize the glycosylated form of all six flagellins better, whereas the antibodies raised against FljK expressed and purified from *E. coli* also efficiently recognizes unglycosylated flagellins.

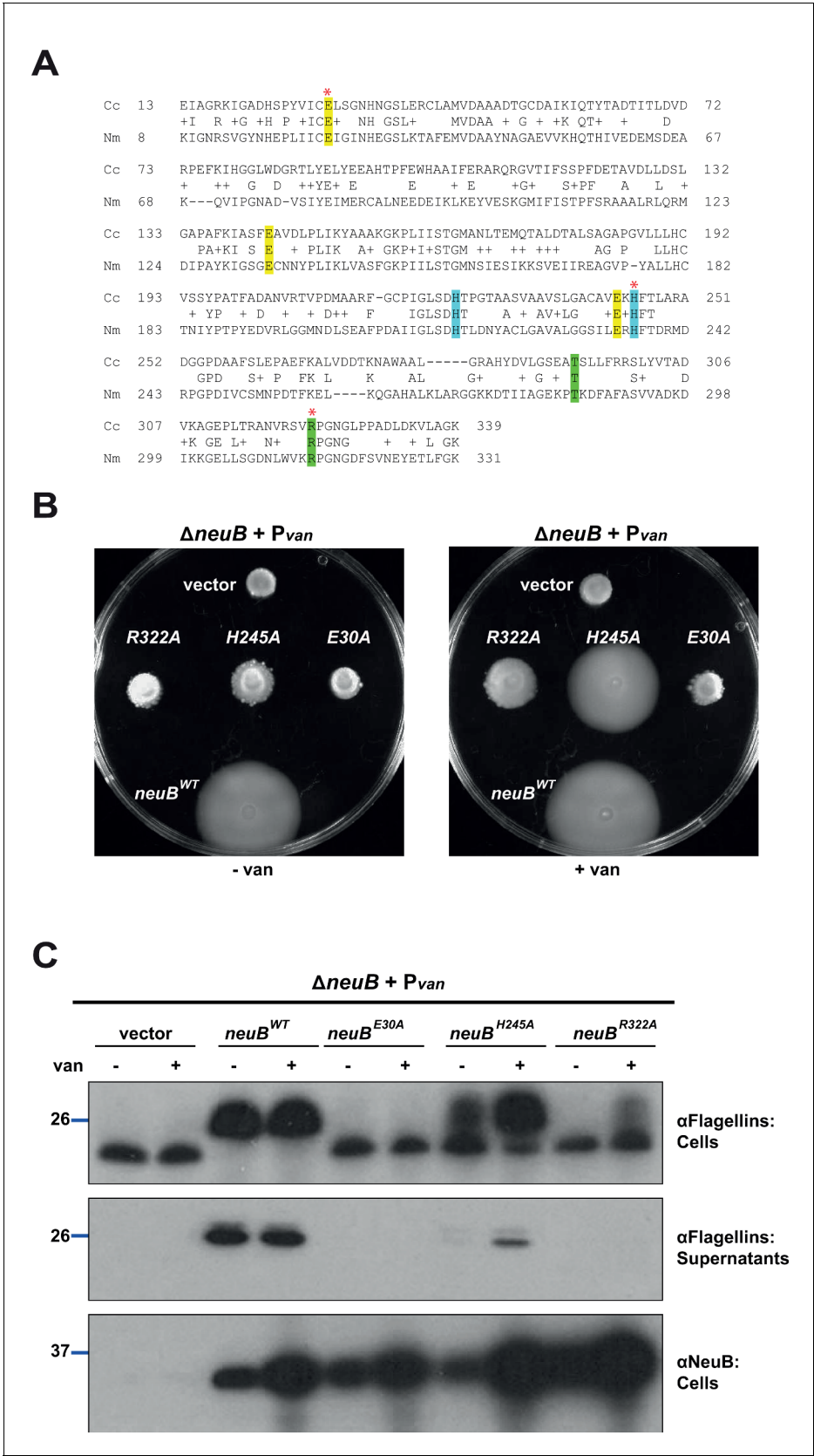


**Figure 2.** NeuB putative catalytic activity is required for motility and flagellin modification. (A) Sequence alignment of *C. crescentus* NeuB (Cc) to *N. meningitidis* sialic acid synthase (Nm). The three glutamate residues that have been proposed to stabilize the reaction intermediate are highlighted in Figure 2 continued on next page

## Figure 2 continued

yellow; the two histidine residues that coordinate the  $Mn^{2+}$  cofactor are highlighted in blue; the threonine and arginine residues highlighted in green are located in the antifreeze-like C-terminal domain and protrude into the active site of the other subunit in the *N. meningitidis* sialic acid synthase dimer. The residues selected for site-directed mutagenesis in *C. crescentus* are indicated by a red asterisk. (B) Motility assay of  $\Delta neuB$  cells complemented with different *neuB* alleles expressed from  $P_{van}$  on a plasmid. Only the WT *neuB* allele can fully complement the motility defect of the  $\Delta neuB$  strain, whereas the allele encoding NeuB(H245A) complements partially and the NeuB(E30A) and (R322A) versions do not restore motility. (C) Immunoblots showing the levels of flagellins and NeuB in  $\Delta neuB$  cells complemented with different NeuB versions expressed from  $P_{van}$  on a plasmid. All the NeuB variants were expressed (lower panel). Immunoblotting for flagellins in whole cell lysates (cells, upper panel) indicates that only the WT NeuB version can restore the migration profile of flagellins, whereas the E30A and R322A variants are inactive and the H245A variant shows an intermediate phenotype. The middle panel shows that only upon induction of the H245A version can the flagellins be detected in the culture supernatant, in agreement with the motility assay shown in panel B. Molecular size standards are indicated by the blue lines, with the corresponding value in kDa. Note that antibodies used in this immunoblot were raised against flagellins purified from *C. crescentus* ( $\alpha$ Flagellins; **Hahnenberger and Shapiro, 1987**) and they detect the glycosylated version of the flagellin better than the other flagellin antiserum ( $\alpha$ FljK, see **Figure 1**).

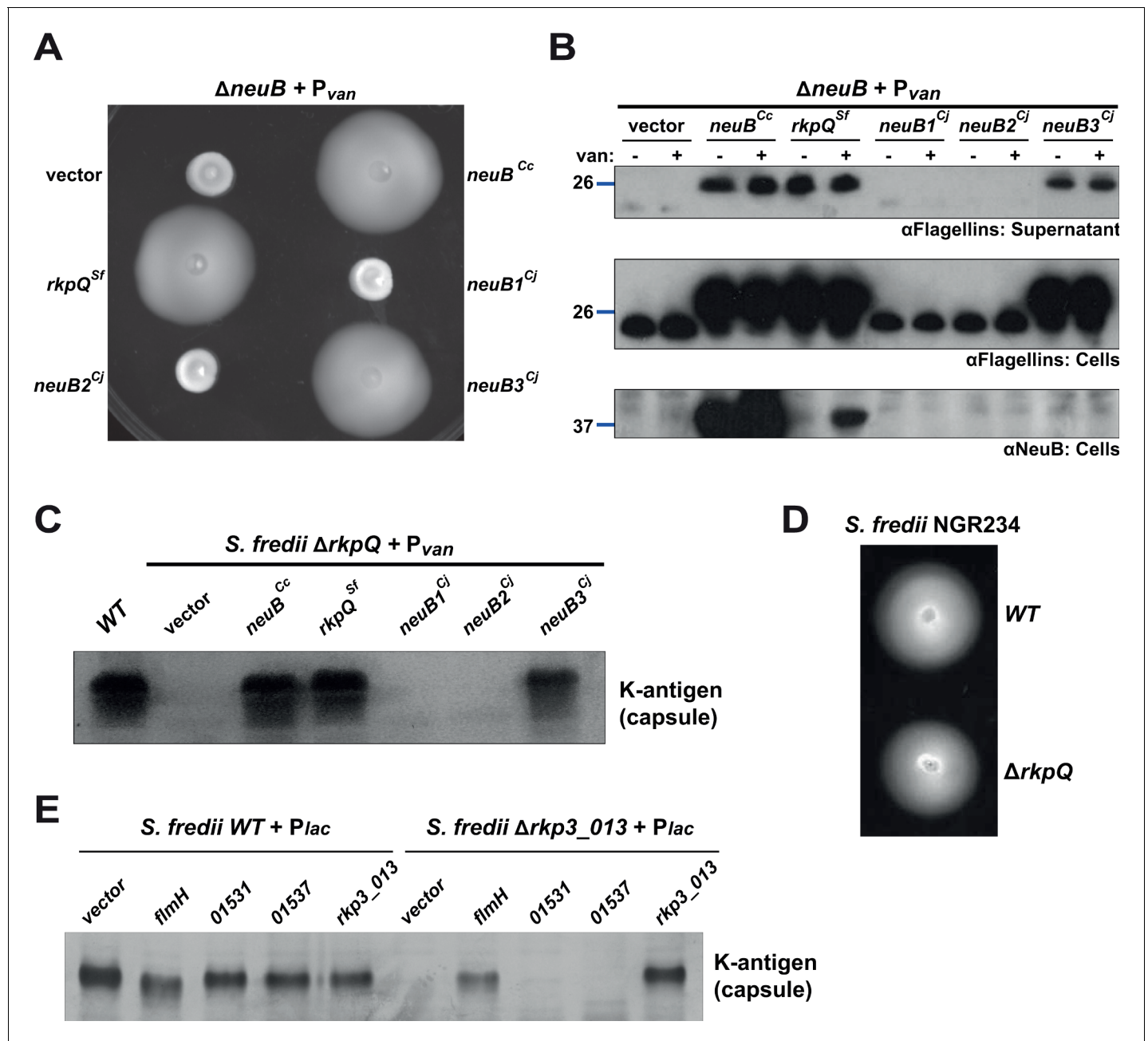


**Figure 3.** Heterologous complementation of the  $\Delta neuB$  mutant with pseudaminic acid synthases. (A) Motility assay of  $\Delta neuB$  cells complemented with different  $neuB$  homologs expressed from  $P_{van}$  on plasmid. Only NeuB from *C. crescentus* and the homologs known to be pseudaminic acid synthases (RkpQ from *S. fredii* and NeuB3 from *C. jejuni*) can fully complement the motility defect of the  $\Delta neuB$  strain, whereas NeuB1 and NeuB2 from *C. jejuni* do not restore motility. (B) Immunoblots showing the intracellular levels of flagellins and NeuB in  $\Delta neuB$  cells complemented with different NeuB homologs expressed from  $P_{van}$  on a plasmid. Consistent with the motility assay shown in panel A, only NeuB<sup>Cc</sup>, RkpQ<sup>Sf</sup>, and NeuB3<sup>Cj</sup> can restore the flagellin migration profile (in whole cell lysates, middle panel) and the secretion of flagellin in the supernatant (upper panel) in  $\Delta neuB$  cells. RkpQ<sup>Sf</sup> is the protein that shows the highest similarity to NeuB<sup>Cc</sup>, as shown by the fact that RkpQ<sup>Sf</sup> is detected by the antibodies against NeuB<sup>Cc</sup> (lower panel). The blue lines on the left indicate the migration of the molecular size standards, with the corresponding value in kDa. Note that antibodies used in this blot were raised against flagellins purified from *C. crescentus* ( $\alpha$ Flagellins; [Hahnenberger and Shapiro, 1987](#)). (C) Capsular polysaccharide profile of *S. fredii* NGR234  $\Delta rkpQ$  mutant cells expressing different NeuB homologs from  $P_{van}$  on a plasmid. Cells with a  $\Delta rkpQ$  mutation do not produce capsular polysaccharide, but production of capsular polysaccharide in  $\Delta rkpQ$  cells can be restored by NeuB<sup>Cc</sup> or NeuB3<sup>Cj</sup> (but not by NeuB1<sup>Cj</sup> or NeuB2<sup>Cj</sup>), which indicates that NeuB<sup>Cc</sup> is a pseudaminic acid synthase. (D) Motility assay of *S. fredii* NGR234 WT and  $\Delta rkpQ$  mutant showing that mutation of the pseudaminic acid synthase does not affect motility in *S. fredii*. (E) Capsular polysaccharide profile of *S. fredii* WT and  $\Delta rkp3\_013$  expressing putative *C. crescentus* acetyltransferases from  $P_{lac}$  on a plasmid. Production of capsular polysaccharide in  $\Delta rkp3\_013$  cells can be restored only by expression of *flmH*, which suggests that FlmH can participate in the pseudaminic acid biosynthetic pathway.

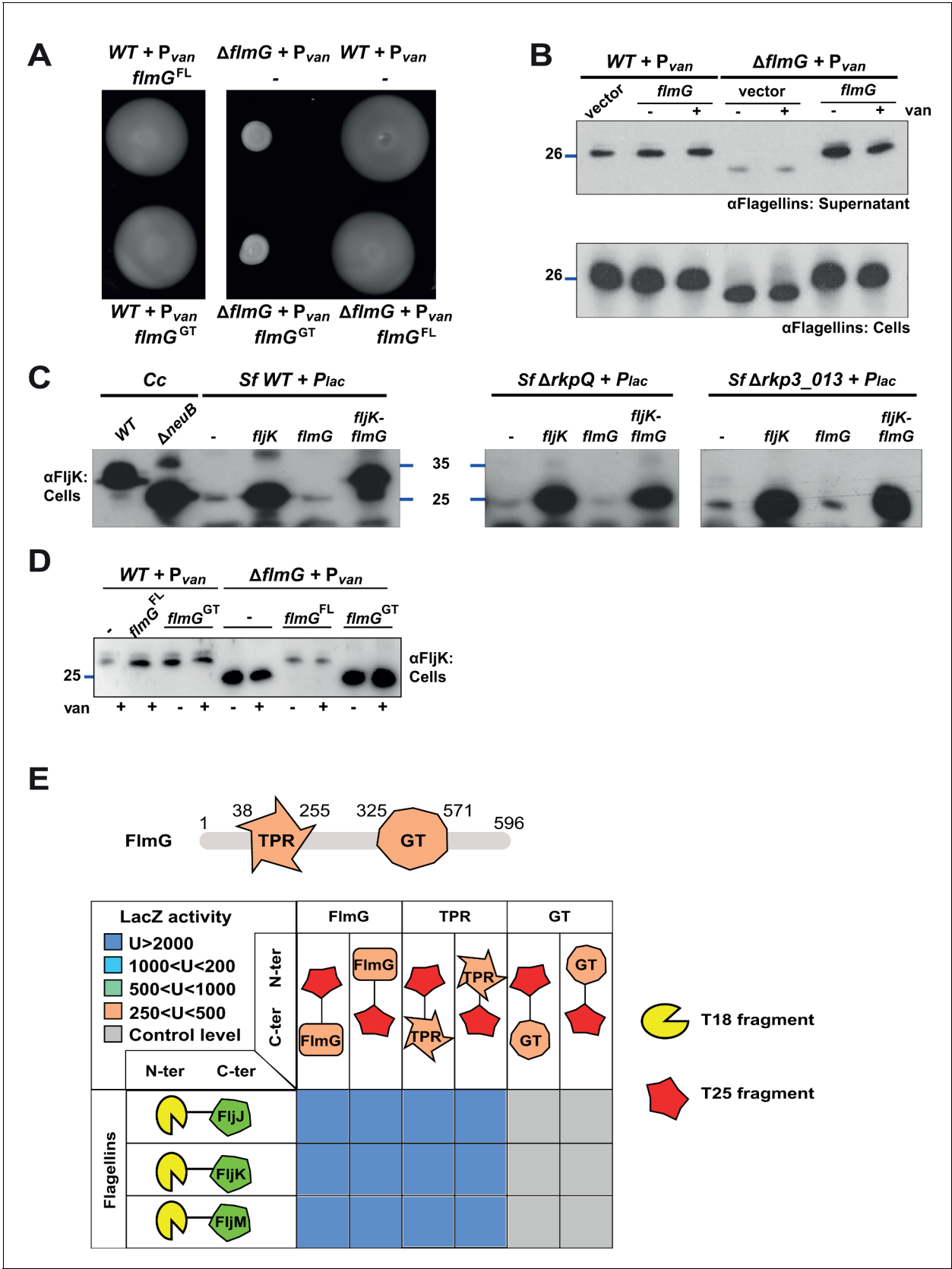


**Figure 4.** FlmG is the putative glycosyltransferase required to post-translationally modify flagellins. (A) Motility assay of WT and Δ*flmG* cells complemented with P<sub>van</sub>-*flmG* full-length (FL) or glycosyltransferase CTD (GT) on plasmid. Δ*flmG* cells are non-motile, as indicated by the compact Figure 4 continued on next page



## Figure 4 continued

swarming. The expression of FlmG full-length from  $P_{van}$  restores motility, in contrast to the GT domain alone. (B) Immunoblot showing the levels of flagellins in supernatants and whole cell lysates from WT and  $\Delta flmG$  cells complemented with  $P_{van}$ -*flmG* on a plasmid. Flagellins produced by  $\Delta flmG$  cells show the same migration profile as those produced by  $\Delta neuB$  cells, with faster migration and reduced abundance in the supernatant. The blue lines on the left indicate the molecular size standard, with the corresponding value in kDa. Note that antibodies used in this blot were raised against flagellins purified from *C. crescentus* ( $\alpha$ Flagellins; **Hahnenberger and Shapiro, 1987**). (C) Immunoblot on *C. crescentus* FljK expressed in *S. fredii* NGR234 strains. The left panel shows that when expressed alone in WT *S. fredii* FljK migrates faster, like in the *C. crescentus*  $\Delta neuB$  mutant. By contrast, co-expression of FlmG and FljK in *S. fredii* NGR234 results in a shift in the migration profile of FljK, similar to that observed in *C. crescentus* WT cells. When FlmG and FljK are co-expressed in *S. fredii* strains unable to synthesize pseudaminic acid ( $\Delta rkpQ$ , middle panel;  $\Delta rkp3\_013$ , right panel) FljK shows only the fast migrating band, independently from the presence of FlmG. The blue lines indicate the molecular size standards, with the corresponding value in kDa. (D) Immunoblot with anti-FljK antibodies on whole cell lysates from WT and  $\Delta flmG$  cells expressing FlmG full-length (FL) or the glycosyltransferase CTD (GT) from  $P_{van}$  on a plasmid. The expression of the GT domain alone does not restore the migration profile of flagellins in  $\Delta flmG$  cells, in agreement with the motility defect shown in panel A. (E) BACTH assay showing the interaction of FlmG with flagellins. The cartoon represents FlmG, with the N-terminal TPR domain and the C-terminal glycosyltransferase domain. The scheme below shows the  $\beta$ -galactosidase activity, expressed in Miller units (U) of *E. coli* BTH101 cells containing the pair-wise combinations of the different constructs used for the BACTH assay. T18 and T25 correspond to the two fragments of the adenylate cyclase and are represented as yellow shape and red star, respectively. Hybrids with the proteins of interest (FlmG, FljJ, FljK, and FljM) were created as N-ter or C-ter fusions, as mentioned. In the case of FlmG, fusions were created with the full-length protein, the TPR domain or the glycosyltransferase (GT) domain only. Gray squares correspond to  $\beta$ -galactosidase activity similar to the control (empty plasmid, U < 250), orange squares indicate an activity between 250 and 500 U, light green squares between 500 and 1000 U, light blue between 1000 and 2000 U, and dark blue above 2000 U. The values of  $\beta$ -galactosidase correspond to the mean and standard deviation of three independent experiments and are listed in **Supplementary file 1** Table S1.



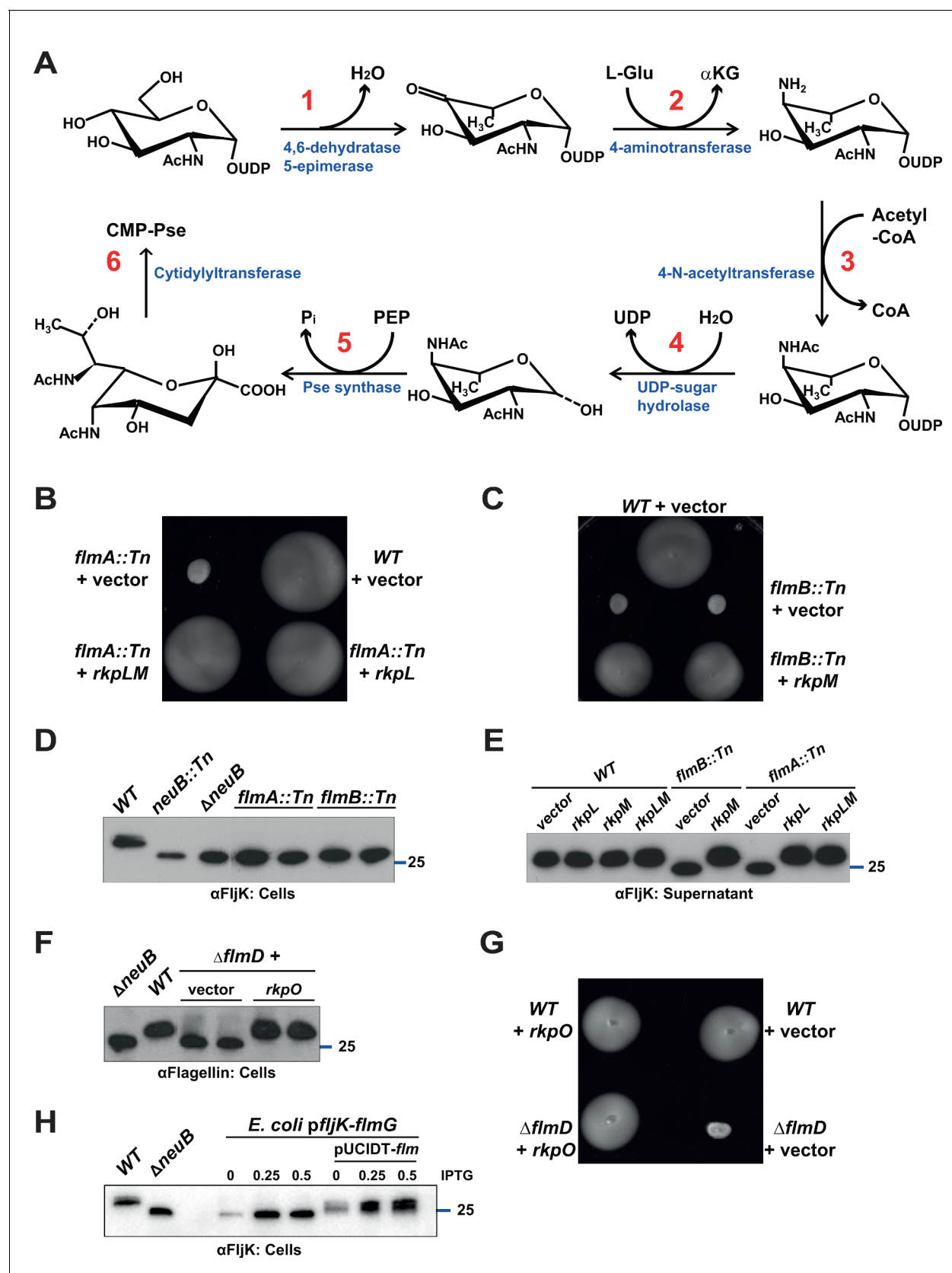


**Figure 5.** Pseudaminic acid biosynthetic pathway in *C. crescentus*. (A) Schematic of the pseudaminic acid biosynthetic pathway as it has been described in *C. jejuni* and *H. pylori* (reviewed in Salah Ud-Din and Roujeinikova, 2018). The different steps are catalyzed by PseB (1), PseC (2), PseH (3), PseG (4), Figure 5 continued on next page

## Figure 5 continued

PseI (5), and PseF (6). (B) Motility assay of WT and *flmA*::Tn cells expressing *S. fredii* NGR234 *rkpL* and *rkpM* from  $P_{van}$  on a plasmid. (C) Motility assay of WT and *flmB*::Tn cells expressing *S. fredii* NGR234 *rkpM* from  $P_{van}$  on a plasmid. (D) Immunoblots of extracts from WT and mutant cells probed with polyclonal anti-FljK antibodies on whole cell lysates. Flagellins produced by *flmA*::Tn and *flmB*::Tn cells show the same migration profile as in  $\Delta neuB$  mutant cells. The blue line indicates the migration of the molecular size standard, with the corresponding size in kDa. (E) Immunoblots of supernatants from WT, *flmA*::Tn and *flmB*::Tn cells probed with polyclonal anti-FljK antibodies. The expression of the *S. fredii* homologs RkpL and RkpM from  $P_{van}$  on a plasmid restores the migration profile and secretion of flagellin in *flmA*::Tn and *flmB*::Tn cells, respectively. The blue line indicates the migration of the molecular size standard, with the corresponding size in kDa. (F) Immunoblot of extracts from WT and  $\Delta flmD$  cells. Mutation of *flmD* impairs post-translational flagellin modification, and the defect is complemented by the expression of the *S. fredii* NGR234 homologue RkpO from a plasmid. The blue line indicates the migration of the molecular size standard, with the corresponding size in kDa. Note that antibodies used in this blot were raised against flagellins purified from *C. crescentus* ( $\alpha$ Flagellins; **Hahnenberger and Shapiro, 1987**). (G) Motility assay of WT and  $\Delta flmD$  cells expressing *S. fredii* NGR234 RkpO from  $P_{van}$  on a plasmid. (H) Immunoblot with anti-FljK antibodies on whole cell lysates from *E. coli* expressing *fljK* and *flmG* from  $P_{lac}$  on a plasmid, in the presence or absence of a compatible plasmid carrying the complete set of *Caulobacter* genes for the pseudaminic acid biosynthetic pathway (pUCIDT-*flm*, see Materials and methods and **Supplementary file 1** Table S3). In the absence of pUCIDT-*flm*, FljK shows the same migration profile as in *Caulobacter*  $\Delta neuB$  cells, whereas in the presence of pUCIDT-*flm* FljK migration is shifted toward higher molecular mass, as in *Caulobacter* WT cells. The values above the panel indicate the concentration of the inducer for  $P_{lac}$ -*fljK*-*flmG* (mM IPTG). The blue line indicates the migration of the molecular size standard, with the corresponding size in kDa.

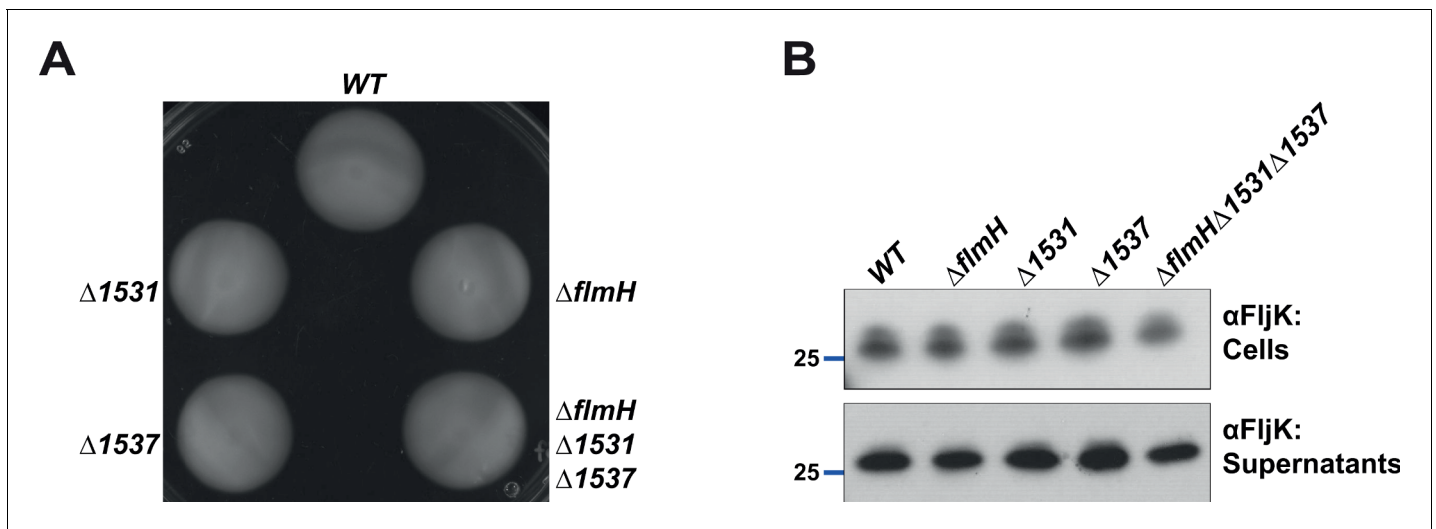


**Figure 5—figure supplement 1.** Acetyltransferase function is likely redundant in *Caulobacter*. (A) Motility assay of strains mutated for the three putative acetyltransferases ( $\Delta flmH$ ,  $\Delta 1531$ ,  $\Delta 1537$ , and the triple mutant  $\Delta flmH \Delta 1531 \Delta 1537$ ). None of the mutants show a motility defect compared to WT cells. (B) Immunoblot with polyclonal anti-FljK antibodies on whole cell lysates and supernatants of strains mutated for the three putative acetyltransferases ( $\Delta flmH$ ,  $\Delta 1531$ ,  $\Delta 1537$ , and the triple mutant  $\Delta flmH \Delta 1531 \Delta 1537$ ). None of the mutants show a defect in flagellins migration or secretion. The blue line indicates the migration of the molecular size standard, with the corresponding size in kDa.

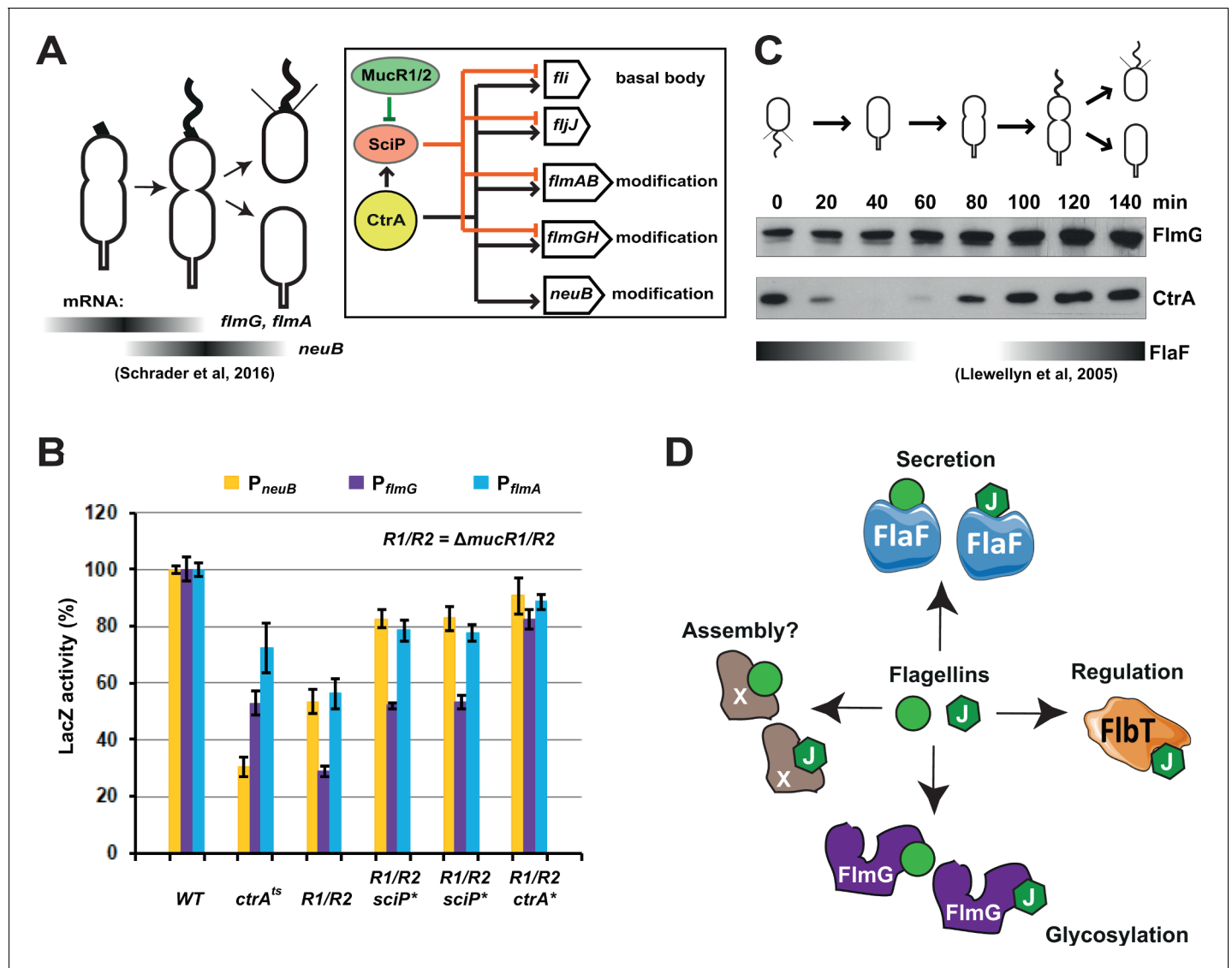


**Figure 6.** Transcription of genes encoding flagellin-modification proteins is cell cycle regulated. (A) Schematic of the transcriptional regulatory network controlling the expression of flagellar and pseudaminic acid biosynthetic genes in *C. crescentus* pre-divisional cells. The gray bars represent the time during the cell cycle when *flmA*, *flmG*, and *neuB* mRNA levels peak (Schrader et al., 2016). The transcriptional regulatory network is represented in the box: CtrA promotes the expression of genes encoding the basal body (*fli* genes), the regulatory flagellin *FljJ* and several components of the flagellin glycosylation pathway (*flmAB* and *flmGH* operons, *neuB*). The expression of these same genes is repressed by SciP (with the exception of *neuB*), whose expression is under control of CtrA (positively) and MucR1/2 (negatively). (B)  $\beta$ -galactosidase activity of  $P_{neuB}$ ,  $P_{flmG}$ , and  $P_{flmA}$  transcriptional fusions. Transcription of *neuB*, *flmG* and *flmAB* is significantly reduced in *ctrA401* (T170I, temperature sensitive allele *ctrA<sup>ts</sup>*) and double  $\Delta mucR1\Delta mucR2$  (*R1/R2*) strains.  $\beta$ -galactosidase activity of  $P_{neuB}$ ,  $P_{flmG}$ , and  $P_{flmA}$  is partially restored in  $\Delta mucR1\Delta mucR2$  cells carrying *ctrA*(T170A), *sciP*(T24I), or *sciP*(T65A) alleles (*ctrA<sup>\*</sup>* and *sciP<sup>\*</sup>*). Values are expressed as percentages (activity in WT NA1000 set at 100%). (C) Immunoblot showing FlmG and CtrA protein levels in synchronized *C. crescentus* cells. The gray bar represents the abundance of the flagellin chaperone FlaF along the cell cycle, as previously shown (Llewellyn et al., 2005). (D) Model depicting a flagellin-centric view of the events during flagellar assembly in *C. crescentus*. The *FljJ* flagellin is illustrated as a green hexagon, whereas the other flagellins (*FljKLMNO*) are depicted as green circles. The events acting on flagellins are translational regulation (binding of *FljJ* by *FlbT*), glycosylation by *FimG*, secretion by *FlaF* and possibly assembly by an unknown factor (X).

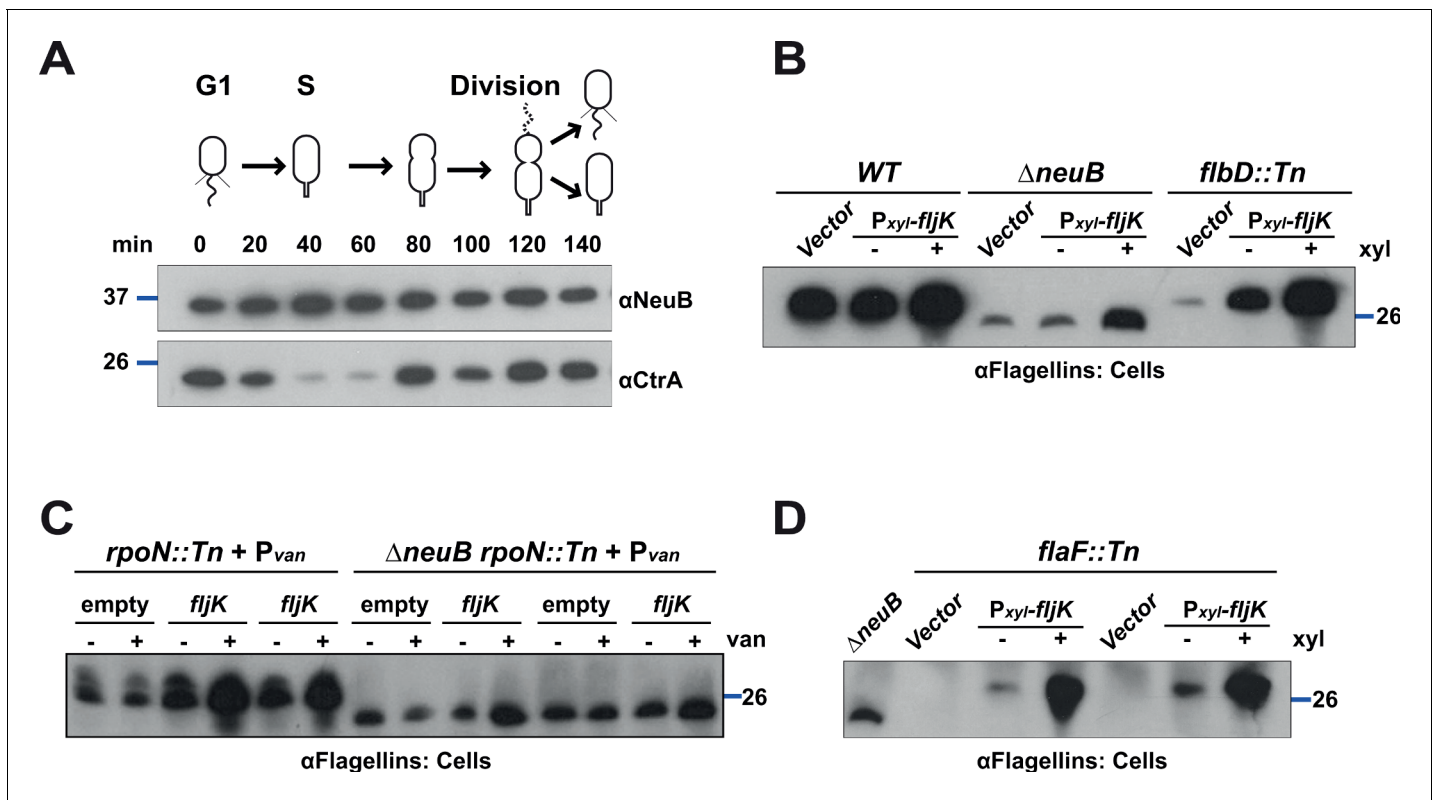


**Figure 6—figure supplement 1.** NeuB is stable along the cell cycle and flagellins can be glycosylated in HBB mutants or in the absence of the FlaF chaperone. (A) Immunoblot showing protein levels in synchronized *C. crescentus* cells: NeuB levels do not change significantly over the cell cycle. The blue lines indicate the migration of the molecular size standards, with the corresponding size in kDa. (B) Immunoblots on WT,  $\Delta neuB$  and  $flbD::Tn$  (lacks the hook, the rings structures in the peptidoglycan and in the outer membrane) cells expressing *fljK* from  $P_{xyl}$  on a plasmid. Upon induction with 0.3% xylose, FljK is produced in  $flbD::Tn$  cells and shows the same migration profile as in WT cells, which indicates that FljK is glycosylated in the  $flbD::Tn$  mutant. The blue line indicates the migration of the molecular size standard, with the corresponding size in kDa. Note that antibodies used in this blot were raised against flagellins purified from *C. crescentus* ( $\alpha$ Flagellins; **Hahnenberger and Shapiro, 1987**). (C) Immunoblot on  $rpoN::Tn$  (lacks the hook, the rings structures in the peptidoglycan and in the outer membrane) and  $\Delta neuB rpoN::Tn$  cells expressing *fljK* from  $P_{van}$  on plasmid. FljK produced in  $rpoN::Tn$  cells shows a migration profile consistent with its modification by glycosylation, compared to  $\Delta neuB rpoN::Tn$  cells. The blue line indicates the migration of the molecular size standard, with the corresponding size in kDa. Note that antibodies used in this blot were raised against flagellins purified from *C. crescentus* ( $\alpha$ Flagellins; **Hahnenberger and Shapiro, 1987**). (D) Immunoblot on  $flaF::Tn$  cells expressing *fljK* from  $P_{xyl}$  on a plasmid. Upon induction with 0.3% xylose, FljK is produced in  $flaF::Tn$  cells and shows the same migration profile as in WT cells, which indicates that FljK is glycosylated in the absence of the FlaF chaperone. The blue line indicates the migration of the molecular size standard, with the corresponding size in kDa. Note that antibodies used in this blot were raised against flagellins purified from *C. crescentus* ( $\alpha$ Flagellins; **Hahnenberger and Shapiro, 1987**).